Electroweak Precision Tests

S. Monteil

Electroweak Precision Tests

Stéphane Monteil
Clermont Université, Université Blaise Pascal,CNRS/IN2P3,
Laboratoire de Physique Corpusculaire, BP 10448, F-63000 CLERMONT-FERRAND,France

This lecture deals with the consistency check of the Standard Model (SM) hypothesis driven by the electroweak precision measurements performed at the Z boson pole (LEP and SLC experiments) and at high energy hadronic machines (Tevatron experiments). Together with the Cabibbo-Kobayashi-Maskawa (CKM) matrix parameters fit, the Z-pole observables consistency check is a pillar of the SM. Following A. Korshin's lecture on SM, we will first describe the free parameters of the SM and introduce the necessity to go beyond the Born approximation. We will hence review the relevant radiative corrections which must be considered as far as the processes at the Z pole are concerned and define which observables can be used to constrain the yet unknown parameters of the SM in the gauge sector. Eventually, we will interpret the global quantum consistency check in terms of the top quark and Higgs masses constraint. The comparison of the predicted and measured top quark mass is a tremendous success of the SM. The prediction of the Higgs mass is driving to a large extent the physics case of the LHC machine.

1 The free parameters of the Standard Model and the necessity of radiative corrections

The electroweak Standard Model [1] has been built in the sixties and received since then fantastic experimental confirmations starting with the observation of the neutral currents by the Gargamelle experiment in 1973, at Cern. The dynamics of the electroweak processes are determined by a gauge symmetry based on the symmetry groups $SU(2)_L \otimes U(1)_Y$, where L is the weak isospin and Y the weak hypercharge. This symmetry must be broken to account for non zero masses of the elementary particles as well as the mediating gauge bosons. This was realised [2] by the introduction of an isospin doublet of scalar fields. Eventually, the SM was proven [3] to be a renormalizable theory at the beginning of the seventies. Let's start this introduction to the necessity of the radiative corrections by a reminder on the free parameters of the SM and the basic relations between them. Following A. Korshin's lecture [4], one might try to categorize the free parameters of this theory:

- The masses of the elementary fermions: though the Brout-Englert-Higgs mechanism allows to introduce non-vanishing masses in the SM Lagrangian, their values are free parameters of the theory and must be determined experimentally. We will see in the next chapters that the heaviest top quark played a particular role. Neutrinos on the opposite side of the masse scale, have been proven to be massive though their masses (or their mass differences) are not measured yet.

- The coupling constants: g_W (weak, charged currents) and $\alpha_{\rm EM}$ (electromagnetic). If I am putting in the game the strong interaction described by the quantum chromodynamics, one needs to consider in addition the strong coupling constant α_S.
- The gauge boson masses: m_W and m_Z.
- The scalar sector: the shape of the scalar potential is basically unknown and is currently expressed thanks to two parameters. Following [2], one might express $V(\Phi) = -\mu^2\Phi^2 + \lambda\Phi^4$, Φ being the scalar fields doublet and λ and μ the parameters of the shape.
- The flavour mixings: after the spontaneous symmetry breaking of the electroweak symmetry, electroweak eigenstates and mass eigenstates can be related through a 3X3 unitary complex matrix. It can be shown that such a matrix is described by four independent parameters, one being a phase, possibly giving rise to CP violation [5]. This is true for quarks but also for leptons as soon as neutrinos are massive (and they are !). Let's add for completeness that there is a further free parameter in the QCD theory, the CP-violating phase θ_S.

The number of free parameters of the SM amounts to 28. Alike elementary fermion masses, the parameters accounting for the flavour mixings are decoupled from the rest of the theory. The interested reader can refer to the lectures about flavour physics and neutrinos physics given in this School [7]. Let's examine how the other free parameters are related.

1.1 Basic relations between free parameters

Though we should try from now on to reduce the problem, I am going to introduce two new parameters: the Fermi coupling constant G_F and the electroweak mixing angle ! G_F is determined from the muon lifetime measurement, and can be expressed as a function of g_W and m_W:

$$G_F = \frac{g_W^2}{4\sqrt{2}m_W^2}. \tag{1}$$

The electroweak mixing angle relates the physical states of electroweak neutral bosons (Z and γ) to the neutral gauge bosons (W_3 and B) of the groups $SU(2)_L$ and $U(1)_Y$:

$$\begin{pmatrix} W_3^\mu \\ B^\mu \end{pmatrix} = \begin{pmatrix} \cos\theta_W & \sin\theta_W \\ -\sin\theta_W & \cos\theta_W \end{pmatrix} \begin{pmatrix} Z^\mu \\ A^\mu \end{pmatrix}. \tag{2}$$

The weak and electromagnetic coupling constants are therefore related through the electroweak angle θ_W:

$$e = g_W \sin\theta_W. \tag{3}$$

It's relevant to choose as free parameters of the theory the very precisely measured G_F and $\alpha_{\rm EM}$ as far as coupling constants are concerned [a]. The electroweak mixing angle will then be used to embody the dependancy on the unknown SM parameters.

[a] The running of $\alpha_{\rm EM}$ up to the Z mass energy scale has to be taken into account and its determination is a masterpiece inside the global electroweak fit.

Going one step further (after the spontaneous electroweak symmetry breaking), the masses of the gauge bosons can be related through the electroweak mixing angle or equivalently by the vacuum expectation value v:

$$m_W = m_Z \cos\theta_W = \frac{1}{2} g_W v. \tag{4}$$

The shape of the scalar potential (previously governed by the μ and λ parameters) can be advantageously described by the mass of the Higgs boson m_H and the vacuum expectation value v which can be expressed thanks to Eq. 1 and Eq. 4 as a function of G_F only.

Eventually, let's introduce the Veltman's parameter:

$$\rho_0 = \frac{m_W^2}{m_Z^2 \cos^2\theta_W} = 1 \ , \tag{5}$$

which measures the ratio of neutral to charged currents in neutrino interactions and is exactly unity at tree level. The vector and axial-vector couplings of the Z boson to fermions will therefore read as:

$$\begin{aligned} g_V &= \sqrt{\rho_0}(I_3 - 2Q\sin^2\theta_W), \\ g_A &= \sqrt{\rho_0} I_3. \end{aligned} \tag{6}$$

Q is the fermion electric charge, I_3 its third component of weak isospin.

Let's summarize: removing the flavour parameters and the masses of the elementary fermions (except top quark, by anticipation), we are left with a set of five independent parameters to be adequately chosen. We already stated that G_F and α_{EM} are very precisely measured. This is the case also for the mass of the Z boson. Those three parameters will from now on be considered as constant within the SM framework [b]. Then the set of unknown parameters to de determined by a global consistency test can be: $\{m_{\mathrm{top}}, m_H\}$.

1.2 Radiative corrections are required

It is possible already right now to make predictions at the tree level within the SM framework. From the relations given Eq. 1 and Eq. 4, the mass of the W boson reads as:

$$m_W = \frac{\pi \alpha_{EM}}{\sqrt{2} G_F} \frac{1}{\sin^2\theta_W}. \tag{7}$$

Provided that G_F is determined from the muon lifetime and $\sin^2\theta_W = 0.228 \pm 0.002$ from the Deep Inelastic Scattering neutrino experiments [9](this choice is made to be independent of the LEP observables including the W mass measurement), one predicts $m_W = 78.1 \pm 0.4$ Gev/c^2. This result has to be compared to the world average measurement $m_W = 80.399 \pm 0.023$ Gev/c^2. They are clearly inconsistent and before rejecting the SM, one should examine the higher order corrections, which are exhibiting in particular loops of virtual particles. They are of three kinds: electromagnetic, QCD and weak. As an example, the diagrams of the QED corrections to the partial width of the Z boson are given in Figure 1.

One is not anymore interested in High Energy Physics in QED nor QCD corrections (the former are well-known and calculable at a level of precision much higher than required by the experimental accuracies). The core subject of the precision electroweak physics is eventually to pin down the weak radiative corrections and prove if it exists an inconsistency between the SM predictions and the measurements.

[b] An interpretation of the data in a different theoretical framework might require to review this statement. For instance G_F will vary significantly in the presence of a fourth fermion generation [8].

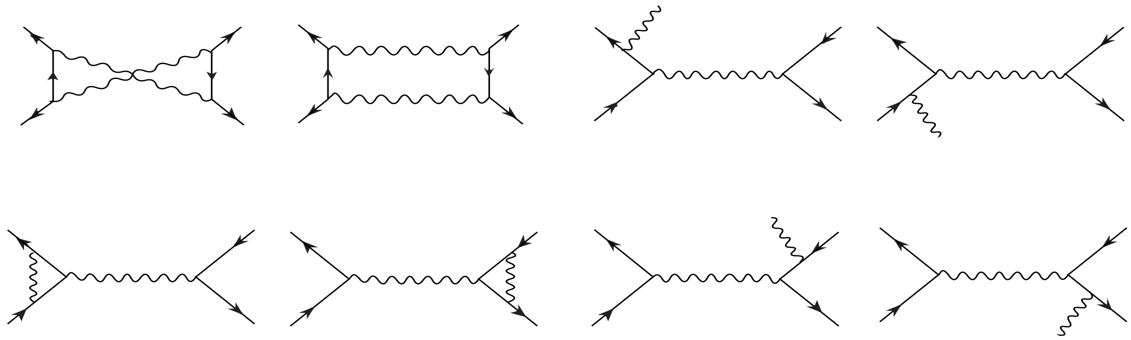

Figure 1: Electromagnetic corrections to the process $e^+e^- \to Z \to q\bar{q}$.

2 The weak radiative corrections

We proved in the section 1 that the Born approximation is not enough to valuably compare measurements and SM predictions. The higher order weak corrections can be sketched in two categories: self-energy and vertex corrections. Focus will be given to the radiative corrections relevant for the Z pole observables.

2.1 Corrections to the propagator

The left part of Figure 2 displays the diagram which are modifying the propagator of the interaction. They are often called self-energy corrections.

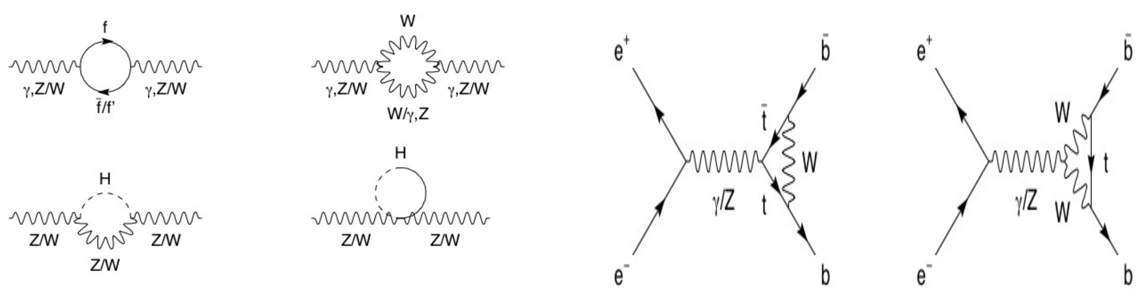

Figure 2: Left diagrams: sketches of radiative corrections to the gauge propagators with one loop diagrams. Right diagrams: vertex radiative corrections

.

They depend on all the particles of the theory and can be translated by the ρ parameter which was previously defined in Eq. 5. Its value is modified to account for the propagator corrections along the form:

$$\rho = \frac{\rho_0}{1 - \Delta\rho}. \tag{8}$$

$\Delta\rho$ depends mainly on $m^2_{\rm top}$ and $\ln(m_H)$. Its current calculation has been performed at the two loops level though one loop is enough with the current experimental precisions. Since the

Z boson couples to loops of virtual fermions proportionally to the squared mass of the fermion, top contributions are dominant as can be seen in Eq. 9.

$$\Delta\rho = \frac{3G_F m_W^2}{8\sqrt{2}\pi^2}\left[\frac{m_{\rm top}^2}{m_W^2} - \tan^2\theta_W(\ln\frac{m_H^2}{m_W^2} - \frac{5}{6})\right] + \text{h.c.}. \tag{9}$$

2.2 Vertex corrections

The diagrams responsible of the vertex corrections are shown in the right plot of Figure 2. The dominant diagram is the production of a virtual top quark pair, which are subsequently weakly decaying. This last transition is proportional to the CKM matrix element $|V_{tq}|^2$. Indeed, the hierarchy of the CKM elements between families within the SM ($|V_{tb}| \approx 1 >> |V_{ts}| \approx 0.04 > |V_{td}| \approx 0.008$) implies that these vertex corrections are only significant for the $Zb\bar{b}$ vertex. They are accounted for by an additional parameter $\Delta\kappa$ which, restraining the expression to $m_{\rm top}^2$ contribution, reads as:

$$\Delta\kappa = \frac{G_F m_{\rm top}^2}{4\sqrt{2}\pi^2} + h.c \tag{10}$$

2.3 A word on QCD corrections

Figure 3 shows the diagrams corresponding to final state strong interaction corrections.

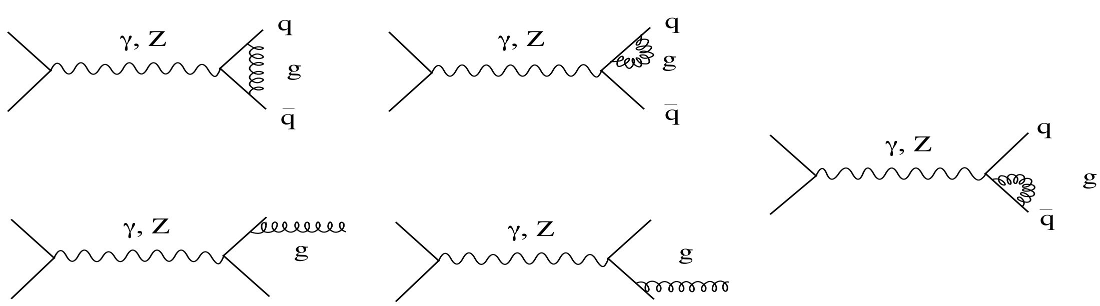

Figure 3: Strong interaction corrections to the process $e^+e^- \rightarrow Zq\bar{q}$.

Contrarily to electromagnetic corrections, the QCD corrections suffer from large uncertainties. The choice of the electroweak observable of interest must be made such that the interpretation of its measurement is not plagued by unmastered QCD effects. For instance, the decay width $\Gamma(Z \rightarrow b\bar{b})$ is subjected to a QCD correction at the level of 4% known to an accuracy of 20%. Hence, one will prefer to measure the partial width $R_b = \frac{\Gamma(Z\rightarrow b\bar{b})}{\Gamma(Z\rightarrow \text{hadrons})}$ for which those corrections are suppressed by a factor 20.

The direction of the quark production is an important experimental measurement as soon as one wants to measure parity violation effects. There, the main source of QCD corrections is the gluon radiation which distorts the initial (electroweak) direction. Calculations of these effects are fully documented in [9] and the references therein.

2.4 Implementation of the radiative corrections

The non-abelian character of the EW symmetry yields triple or quadrilinear couplings of intermediate bosons. These couplings reflect in the radiative corrections. Hence, we might access to the hidden part of the SM (and more generally to NP) at the Z pole energy scale. As previously stated, the kinematically forbidden excitations at the Z energy (top quark, W and Higgs bosons) will appear predominantly into the virtual particle loops.

What is modified ? At first glance, the numerical predictions of course but also the relations between parameters or their definitions themselves. On top of that, the predictions must be renormalized to compensate possible infinities induced by these corrections. The renormalization is realized through a redefinition of the parameters of the lagrangian and the fields. Since not all orders of corrections are accounted for, the final prediction should depend upon the renormalization scheme. We will follow here the prescription adopted by the LEP ElectroWeak Working Group (LEPEWWG): the renormalization scheme used in the EW precision fit is the on-shell scheme (QED driven) where:

- The physical masses are the pole propagators.
- The EM coupling constant is the fine structure constant.
- The weak mixing angle is defined according to Eq. 4 where the physical masses of the gauge bosons are considered.

In practice, one keeps the functional form of the tree-level equations which we have written in Section 1 and uses an ad-hoc operatorial change of variables to be applied to the theroretical expression of any observable:

$$\begin{aligned} \sin^2\theta^f_{\text{eff}} &= \kappa_f \sin^2\theta_W, \\ g^f_V &= \sqrt{\rho_f}(I^f_3 - 2Q\sin^2\theta^f_{\text{eff}}), \\ g^f_A &= \sqrt{\rho_f} I^f_3, \end{aligned} \tag{11}$$

where κ_f and ρ_f embody the propagator and vertex corrections previously defined such that:

$$\begin{aligned} \kappa_f &= 1 + \Delta\kappa_f, \\ \rho_f &= 1 + \Delta\rho_f. \end{aligned} \tag{12}$$

The parameters κ_f and ρ_f contains each propagator (self-energy) and vertex radiatve correction. The former is universal, the latter is flavour-dependent. A more expanded and maybe more readable form is for instance $\rho_f = 1 + \Delta\rho\ (\mathrm{self-energy})\ + \Delta\rho_v\ (\mathrm{vertex})$.

3 The Z pole observables

In order to cope with the required number of pages dedicated to this lecture, I will only briefly define the main observables of interest and skip the description of the measurement techniques. The interested reader can get some details of the measurements in the lecture slides.

An illustrative example of the quest to prove genuine weak radiative corrections is the measurement of the partial decay width of the Z boson in pairs of b quarks. The measurement of the ratio $R_b = \frac{\Gamma(Z\to b\bar{b})}{\Gamma(Z\to \mathrm{hadrons})}$ makes it less sensitive to QCD corrections. Conversely, since the weak propagator corrections are universal, they are also suppressed. This observable is hence solely sensitive to the weak vertex corrections. The tree-level Rb prediction can be compared to the prediction including radiative corrections:

$$\begin{aligned} R_b &= 21.83\%\ \mathrm{tree-level}, \\ R_b &= 21.58 \pm 0.02\%\ \text{with}\ m_{top} \approx 170\mathrm{GeV}. \end{aligned} \tag{13}$$

The experimental challenge in order to probe the vertex corrections is then to reach a precision of the measurement better than the percent level. The statistics is not an issue here:

the devilish part is the control of the systematics linked to the tagging of the beauty quarks. From the very first measurement towards the final word of the LEP experiments, the precision of the R_b measurement improved from 5% to 0.3% and the value reads as:

$$R_b = 21.644 \pm 0.064\%, \tag{14}$$

in very satisfactory agreement with the existence of an heavy top quark, if the SM is realized in the Nature.

Another class of important measurements are the parity violating asymmetries at the Z pole, allowing to access the universal propagator corrections interpreted in terms of $\sin^2\theta_{\text{eff}}$. Since parity is maximally violated in the weak interaction, the fermion issued from the Z decay is produced preferentially in the direction of the incoming fermion. Let's start with unpolarized electron beams. One can define a forward-backward production asymmetry of final state fermion such as:

$$A_{\text{FB}}^{f\bar{f}} = \frac{N_{\text{F}} - N_{\text{B}}}{N_{\text{F}} + N_{\text{B}}}, \text{ with } N_{\text{F}} = \int_0^1 \frac{d\sigma^{f\bar{f}}}{\mathrm{d}\cos\theta}\mathrm{d}\cos\theta. \tag{15}$$

$\sigma^{f\bar{f}}$ is the fermion-antifermion cross-section and θ the production angle of the fermion relative to the incoming electron. It is straightforward to derive the asymmetry as a function of the weak neutral current coupling constants:

$$A_{\text{FB}}^{f\bar{f}} \propto \frac{g_V^e g_A^e}{(g_V^e)^2 + (g_A^e)^2} \cdot \frac{g_V^f g_A^f}{(g_V^f)^2 + (g_A^f)^2}) \propto A_e \cdot A_f, \tag{16}$$

showing that $A_{\text{FB}}^{f\bar{f}}$ depends primarily on $\sin^2\theta_{\text{eff}}$, when replacing the coupling constants written in Eq. 6.

It is then interesting to calculate the derivative of $A_{\text{FB}}^{f\bar{f}}$ and A_f as a function of $sin^2\theta_{\text{eff}}$. The most sensitive observables are found to be A_e and $A_{\text{FB}}^{d\bar{d}}$ where d stands for any quark of type down. The clearer experimental signature for down-type quarks is obtained for b quarks because of the kinematical and topological characteristics linked to its high mass and relatively long lifetimes of b-hadrons. A_e and $A_{\text{FB}}^{b\bar{b}}$ are therefore the golden-plated observables for the electroweak precision test. As an illustration of the forward-backward asymmetry of heavy quarks determination, Figure 4 shows in particular the observed angular distribution of the outgoing fermion in the Aleph experiment. The average of all b-asymmetries at LEP is $A_{\text{FB}}^{b\bar{b}} = 0.0992 \pm 0.0016$, yielding $\sin^2\theta_{\text{eff}} = 0.23221 \pm 0.00029$.

If A_{FB} can be measured at LEP and SLD, the measurement of A_e (asymmetry in the initial state of the reaction $e^+e^- \to Z \to f\bar{f}$) can only be performed at SLD machine, where the electron beam was polarized. A simple counting experiment can therefore be designed: let N_L be the number of Left-Handed $e_L^+e_L^- \to Z$ and N_R the number of Right-Handed $e_R^+e_R^- \to Z$; one can build the asymmetry A_{LR}:

$$A_{\text{LR}} = \frac{N_L - N_R}{N_L + N_R} \cdot \frac{1}{\langle P_e \rangle}, \tag{17}$$

with $\langle P_e \rangle = 0.7292 \pm 0.0038$ the polarization fraction of the electron beam. A_{LR} is measured to be: $A_{\text{LR}} = 0.1514 \pm 0.0022$, the precision being completely dominated by the polarization measurement. Conversely, the derivation of $\sin^2\theta_{\text{eff}}$ yields: $\sin^2\theta_{\text{eff}} = 0.23097 \pm 0.00027$. This measurement is only in marginal agreement with the one issued from the b-asymmetry.

To conclude this Section, Figure 5 summarizes in a single table all the measurements which are taken into account in the global electroweak fit. By anticipation of the next Section, the SM predictions of these observables as derived from the global fit are given together with the measure of their consistency within the overall SM picture.

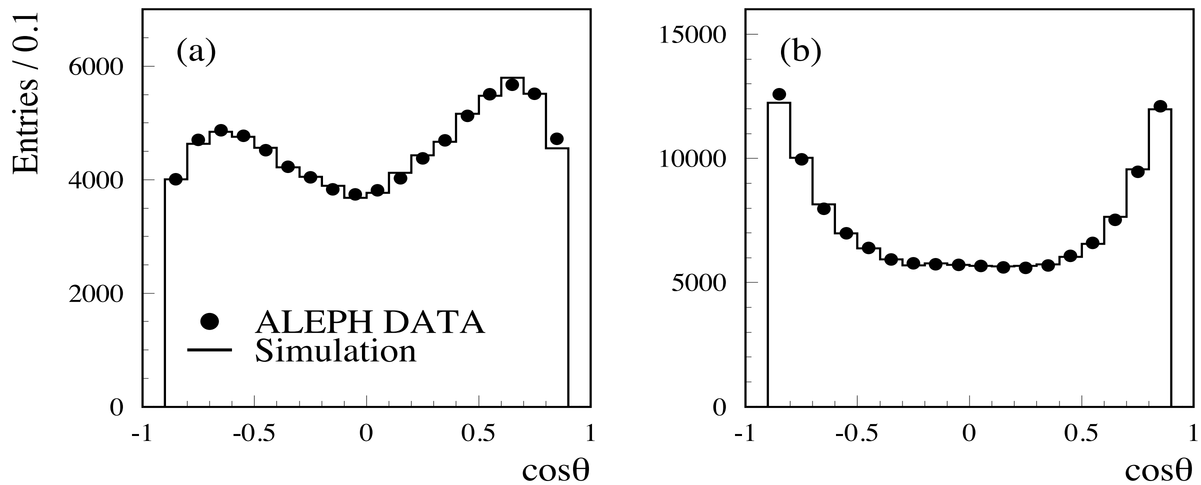

Figure 4: Observed angular distribution of the fermions in the Aleph experiment in a) a sample enriched in b-events, b) a sample enriched in charm events. The histogram displays the SM prediction by means of simulated Monte-Carlo events.

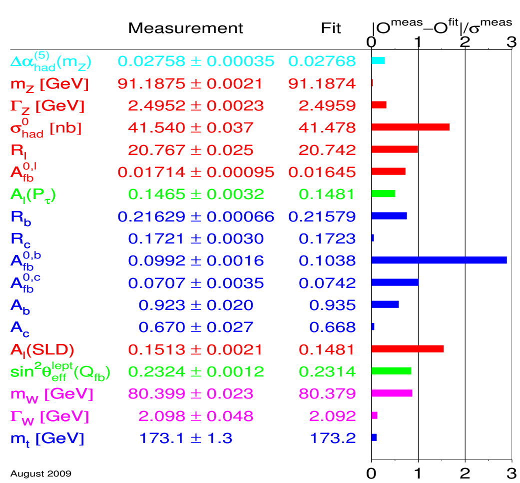

Figure 5: Numerical comparison of measurements and predictions (as derived from the global electroweak fit) for 18 electroweak observables. Their agreement is qualified with a pull.

4 The global consistency check of the Standard Model

As exposed in Section 2, the quantity $\sin^2\theta_{\rm eff}$ endorses the weak radiative corrections to the Z propagator and depends on the top quark and Higgs boson mass, quadratically and logartihmically, respectively. It is hence possible to interpret its measurement in terms of constraints on the two fundamental parameters $m_{\rm top}$ and m_H. The comparison of $m_{\rm top}$ derived from Z pole observables to the direct measurement at Tevatron is the first interpretation we will examine. By anticipation, it is certainly a pillar of the SM. More interestingly for the immediate future of High Energy Physics is the indirect constraint on the Higgs boson mass. It is so far the most grounded knowledge we got of the scalar sector of the SM.

The LEPEWWG performed the extraction of $\sin^2\theta_{\rm eff}$ from all the relevant observables measured at LEP and SLC experiments. Namely it consists of the forward-backward asymmetries of heavy quarks (c and b), the leptonic Left-Right asymmetry with the polarized beams of the SLC accelerator, the τ lepton polarization and the leptonic forward-backward asymmetries, which were briefly reviewed in Section 3. This list of observables is written in decreasing precision on $\sin^2\theta_{\rm eff}$ as indicated in Figure 4.

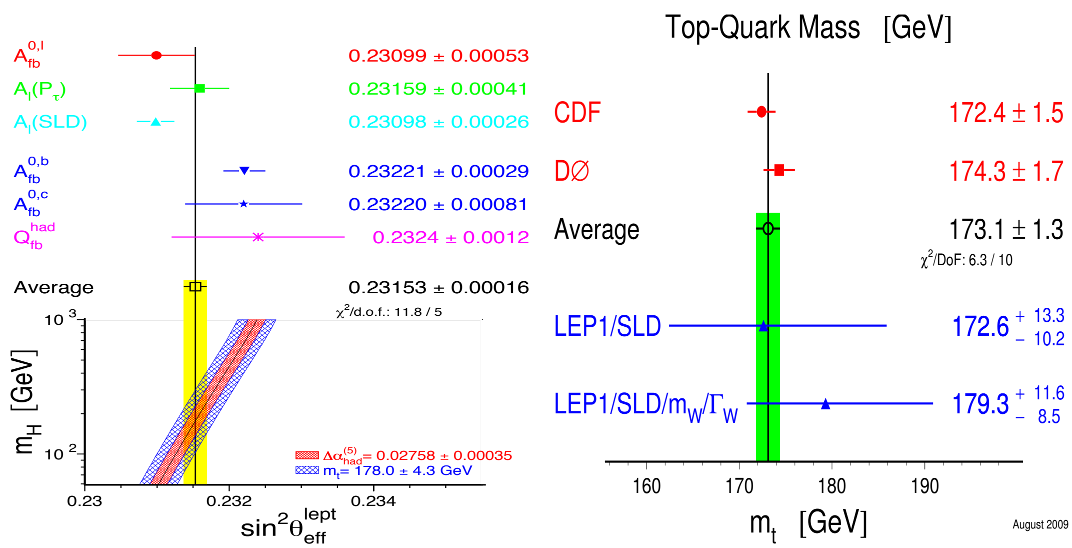

Figure 6: Left plot: the set of measurements which give access to the electroweak mixing angle. The dependencies on the top quark and Higgs boson mass are indicated. Right plot: direct and indirect determinations of the top quark mass.

In addition, the partial width R_b and R_c, the hadronic cross-section of the Z boson into hadrons, $\sigma^0_{\rm had}$, and the ratios of Z decay widths into hadrons to leptons, R_ℓ are considered in the global consistency check. Eventually, the masses and widths of the Z and W bosons as well as the measured top quark mass are completing the list of inputs entering into the global fit.

A first comment is in order. What is done here is a statistical test of the consistency of the SM prediction and the corresponding measured observables. The quality of the fit is measured with a χ^2 per degree of freedom: it is found to be $\chi^2/{\rm d.o.f} = 1.40$, which corresponds to a probability value of 15%. The SM hypothesis passes the electroweak precision test! It is hence legitimate to make the metrology of the parameters.

Let's start by the extraction of $m_{\rm top}$. Figure 4 (right plot) gathers its direct and indirect determinations. The former are realized by the two Tevatron experiments (LHC will come soon); the latter are split according to two fit scenarii: the first one is coming solely from the interpretation of $\sin^2\theta_{\rm eff}$ and R_b measurements, the second contains in addition the W mass and width measurements. I should add that the "LEP and SLD" prediction of $m_{\rm top}$ was obtained prior to the discovery of the top quark. The agreement between direct and indirect determinations is definitely remarkable and constitutes a tremendous success of the Standard Model.

$$\begin{aligned} m_{\rm top} &= 173.1 \pm 1.3 \;\; {\rm Gev}/c^2, [({\rm direct} - {\rm Tevatron})] \\ m_{\rm top} &= 172.6 \,{}^{+13.3}_{-10.2}\; {\rm Gev}/c^2 \; [({\rm indirect} - {\rm LEP1})]. \end{aligned} \tag{18}$$

It is possible to play the exact same game with the W boson mass. It might appear less impressive because the W boson was already discovered. Yet, in the light of the tree-level prediction we performed in the Section 1, the again remarkable agreement which is observed and sketched in Figure 7 is another proof of the relevance of genuine weak radiative corrections.

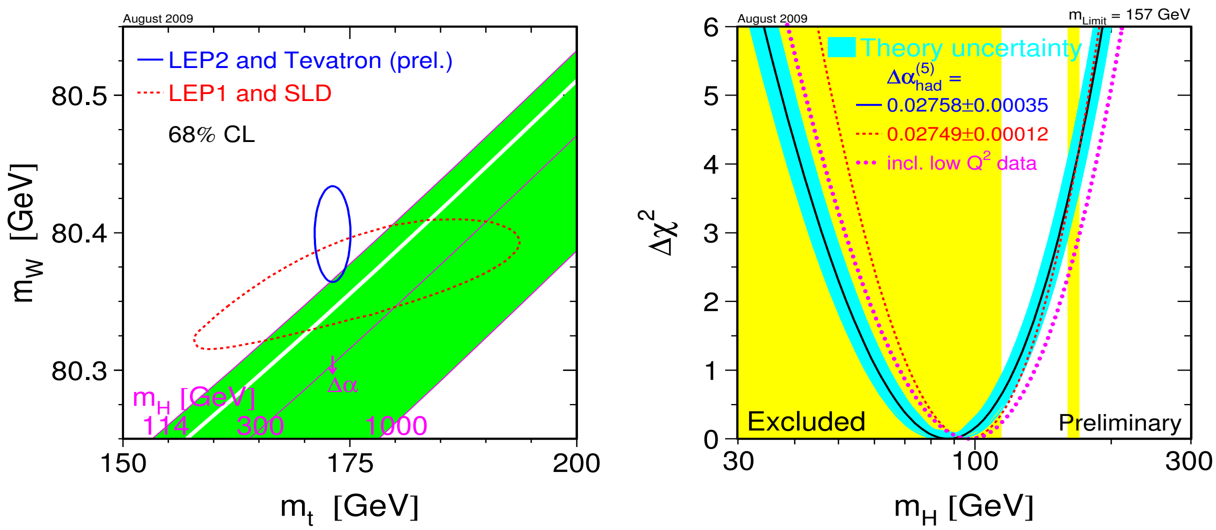

Figure 7: Left plot: the W boson mass as a function of the top quark mass. The red curve represents the predictions at 68 % CL derived from the global consistency check of the SM. The blue curve is the contour at 68 % CL of the direct measurements performed at LEP2 and at Tevatron. The green band shows how the Higgs boson mass depends on $m_{\rm top}$ and m_W. Right plot: Prediction of the mass of the Higgs boson as a result of the global consistency check of the Z pole observables, the W boson mass and the top quark mass.

Though the logarithmic dependancy of the observables $\sin^2\theta_{\rm eff}$ and m_W on the mass of the Higgs boson, it is possible to constrain m_H with a precision which, far from being satisfactory, makes it anyway the most solid information we currently have on the Higgs boson. Figure 7 displays the most probable value of the Higgs boson mass as preferred by the combined electroweak precision measurements. The indirect determination of the Higgs mass reads:

$$m_H = 87 \,{}^{+35}_{-26}\; {\rm GeV}/c^2. \tag{19}$$

A more adequate writing regarding the precision of this determination is:

$$m_H < 157 \; {\rm GeV}/c^2 \; @95\% \; {\rm CL}. \tag{20}$$

The limit on the Higgs boson mass issued from its direct searches is indicated on Figure 7 and reads as $m_H > 114$ GeV/c^2 at 90 % CL. It stands in the range of the electroweak precision measurements preferred region. Recent searches at Tevatron of bosonic decays of the Higgs boson allowed to further exclude at 90 % CL a region close to the kinematical threshold of the decay $H \rightarrow W^+W^-$. The discovery of a light Higgs boson at the LHC experiments would be an outstanding success of both the SM and the LHC. It would also be a retrospective success of the LEP and SLD experiments.

5 Conclusions

The construction of the unified electroweak theory at the end of the sixties changed the landscape and the perspectives of the High Energy Physics. Thirty years later, at the closure of the twentieth century, the LEP machine and experiments produced a fantastic consistency check of the Standard Model, which raises a single fundamental question: what is the underlying mechanism of the electroweak symmetry breaking ? Somehow, we are not far from the formulation of the main question raised at the end of the nineteenth century: what is the vacuum made of ? If it happens that the Nature has chosen to fill the vacuum with Higgs bosons, the very near future of the LHC machine and experiments will tell.

Acknowledgments

Most of the materials reproduced here are issued from the LEP and Tevatron Electroweak Working Group web page. I would like to warmly thank the students of this school for the stimulating interactions they provoked and the excellent spirit which accompanied this school. I'd like also to express a friendly thought to the professors and organisers team.

References

1. S. Glashow, *Nucl. Phys.* B **20**, 579 (1961). S. Weinberg, *Phys. Rev. Lett.* **19**, 1264 (1967). A. Salam, in Elementary Particle Theory, ed. N. Svartholm (1968).
2. F. Englert and R. Brout, *Phys. Rev. Lett.* **13**, 321 (1964). P. Higgs, *Phys. Lett.* B **12**, 132 (1964); P. Higgs, *Phys. Rev. Lett.* **13**, 508 (1964).
3. G. 't Hooft and M.Veltman, *Nucl. Phys.* B **44**, 50 (1972).
4. A. Korshin, Lecture on the Standard Model, these proceedings.
5. M. Kobayashi and T. Maskawa, *Prog. in Th. Phys.* **49**, 652 (1973).
6. D. Pirjol, Lecture on New Physics, these proceedings.
7. M-H. Schune, Lecture on Flavour Physics and CP violation, these proceedings.
   A. Zalewska, Lecture on Neutrino Physics, these proceedings.
8. H. Lacker and A. Menzel, arXiv:1003.4532v2.
9. The Aleph, Delphi, L3, Opal Collaborations, the LEP Electroweak Working Group and the SLD Electroweak and Heavy Flavour Groups, "Precision Electroweak Measurements on the Z Resonance", Physics Reports: Volume **427** Nos. 5-6 (May 2006) 257-454.
10. The Tevatron Electroweak Working Group, for the CDF and D0 collaborations, [hep-ex:0903:2503].